

Small Calculus Detection for Medical Acoustic Imaging Using Cross-Correlation between Echo Signals

Hirofumi Taki, Takuya Sakamoto, Toru Sato
 Graduate School of Informatics
 Kyoto University
 Kyoto, Japan
 hirofumi.taki@mb6.seikyou.ne.jp

Makoto Yamakawa
 Advanced Biomedical
 Engineering Research Unit
 Kyoto University
 Kyoto, Japan

Tsuyoshi Shiina
 Graduate School of Medicine
 Kyoto University
 Kyoto, Japan

Abstract—Small calculus detection is important to differentiate malignant from benign masses. Although ultrasonography has an excellent ability to depict soft tissue, it plays a secondary role in detection because of its poor calculus sensitivity compared with computed tomography and other X-ray tests. In this paper, we propose a novel method to detect small calculi using cross-correlation coefficients between IQ data of adjacent scan lines. Results of an experimental study show that the proposed calculus detection method has the potential to depict small calculi about 0.3 mm in diameter.

Keywords—Ultrasonography; calculus; correlation; CT; CFAR

I. INTRODUCTION

Ultrasonography (US) has an excellent ability to depict soft tissue without ionizing radiation [1, 2], and thus has been used widely on clinical placement. However, the detectability of US for small calculi is insufficient compared with computed tomography (CT) and other X-ray tests. As a result, US often plays a secondary role when making distinctions between malignant and benign masses. Therefore the improvement of US in calculus detection is strongly desired to serve a convenient and effective imaging tool.

The echo scattered from a calculus has high intensity, and thus one strategy to detect calculi is to extract regions with high echo intensity in a B-mode image. This problem is equivalent to detecting targets in unstable noise and clutter while maintaining a constant probability of false alarm. To solve this problem, Finn et al. and Hansen et al. designed cell averaging constant false alarm rate (CA CFAR) detectors to set a threshold adaptively according to local noise levels [3, 4]. CA CFAR detectors have been employed for target detection in inhomogeneous medium [5, 6]. However, the echo intensity scattered from a small calculus is weak compared with that of a specular echo, indicating that this strategy is not suitable for small calculus detection.

Tissue harmonic imaging (THI) improves contrast resolution of US by suppression of speckle artifacts [7, 8]. The calculus detectability of THI is higher than that of conventional US; however, THI has a considerably low sensitivity compared

with CT and other X-ray tests. By contrast, spatial compound imaging constructs a single B-mode image from multiple sweeps [9, 10]. This technique suppresses acoustic shadowing, one of the essential components to detect calculi. Therefore, spatial compound imaging is inappropriate for calculus detection.

In this study, we propose a novel calculus detection method using correlation coefficients between IQ data of adjacent scan lines, and experimentally verified the potential of the proposed method to detect small calculi about 0.3 mm in diameter.

II. METHODS

The proposed calculus detection method employs the cross-correlation coefficients between raw ultrasound in-phase and quadrature (IQ) data of adjacent scan lines behind a measurement point. When a calculus exists in a transmit beam, the waveform of a transmit pulse changes considerably. Therefore, the echo waveform of a scan line with a calculus is quite different from that without a calculus, where the echoes return from a range behind the calculus. Fig. 1 shows the schema of this process. We can presume the existence of a calculus from a decrease in cross-correlation coefficients. The correlation coefficient behind a measurement point with a Wiener filter is expressed as follows:

$$G(x, z, l) = \frac{\left| \sum_{z'=z_1}^{z_2} g(x, z') g(x + \Delta X, z' + l\Delta Z) \right|^*}{\sqrt{\sum_{z'=z_1}^{z_2} |g(x, z')|^2 \sum_{z'=z_1}^{z_2} |g(x + \Delta X, z' + l\Delta Z)|^2}}, \quad (1)$$

where x and z are the lateral and vertical components, respectively, of a measurement point on a B-mode image, $g(x, z)$ is the IQ datum at $P(x, z)$, a pixel in a B-mode image, $g(x, z)^*$ is the conjugate of $g(x, z)$, ΔX is the interval of scan lines, ΔZ is the range interval, z_1 and z_2 are the minimum and maximum of the z coordinates of a correlation window behind $P(x, z)$.

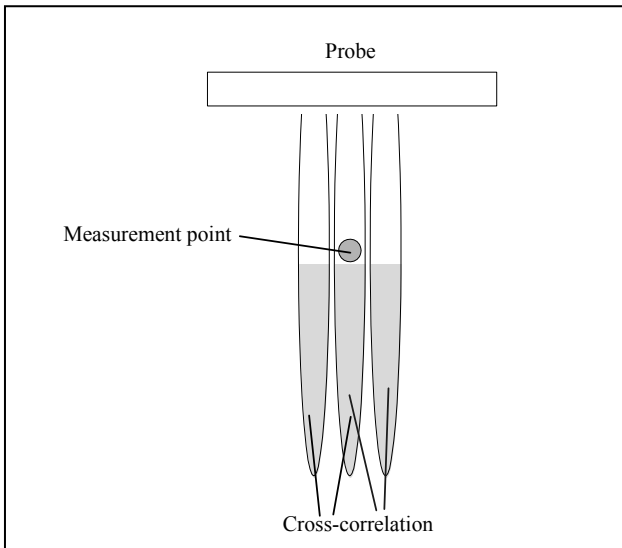


Figure 1. Cross-correlation between IQ data of adjacent scan lines.

A correlation coefficient is suppressed by not only a calculus, but also noise. When signals cut out by correlation windows have low signal-to-noise ratio (SNR), the effect of noise on the correlation coefficients is emphasized, interfering with the detection of the decrease on correlation coefficients originated by a calculus. In this study, we employed a modified Wiener filter to suppress the influence of noise on cross-correlation coefficients calculated by the proposed method. The cross-correlation coefficient with a modified Wiener filter is expressed as follows:

$$r(x + \frac{\Delta X}{2}, z) = \frac{\left| \sum_{z'=z_1}^{z_2} g(x, z')g(x + \Delta X, z' + L\Delta Z)^* + N \right|}{\sqrt{\sum_{z'=z_1}^{z_2} |g(x, z')|^2 \sum_{z'=z_1}^{z_2} |g(x + \Delta X, z' + L\Delta Z)|^2 + N}} \quad (2)$$

$$N = \alpha I_t \quad (3)$$

Where N is a constant to raise a cross-correlation coefficient to 1 when the echo intensity cut out by a correlation window is low, α is a real number and I_t is the signal intensity at 0.5% from the maximum. L is equal to l when the correlation coefficient behind a measurement point, $G(x, z, l)$, is maximum.

III. CALCULUS PHANTOM SETUP

A. Calculus Phantom

When a layered structure exists just behind a calculus, specular echoes scattered from the layered structure interfere with the detection of the calculus. To investigate the effect of the proposed calculus detection method in a severe condition mentioned above, we prepared a calculus phantom with a layered structure, as shown in Fig. 2. Three copper wires 0.2, 0.29 and 0.4 mm in diameter were embedded in an agar gel block at 2 cm depth at 1 cm intervals. A polyethylene sheet 0.1 mm thick was positioned closely behind the wires. The Agar

gel contained 0.5% spherical polymer particles 7 μm in diameter (Tech Polymer; Sekisui Plastics Co., LTD.).



Figure 2. Calculus phantom utilized in this study.

B. Acoustic Imager

We utilized IQ data exported from a commercial medical acoustic imager (EUB-8500; Hitachi Co. LTD.). US was performed with a linear array probe, where the scan line interval was about 0.13 mm and the center frequency of a transmit pulse was 7.5 MHz.

IV. RESULTS

A. Calculation of N

Figure 3 shows the intensity distribution of a B-mode image. We assumed that the average noise intensity of an IQ datum of a pixel is I_t when noise intensity is maximum in a signal cut out by a correlation window. To raise the correlation coefficient to 0.8 in the case that SNR is 0 and average noise intensity is I_t , we set N as $4HI_t$, where H is the number of pixels in a signal cut out by a correlation window.

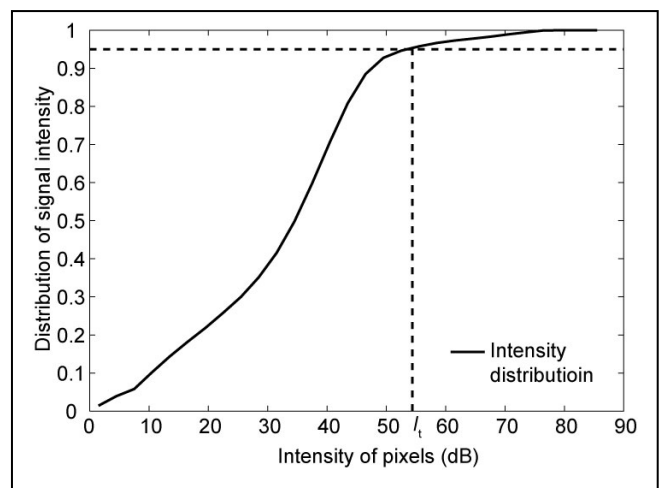


Figure 3. Intensity distribution of a B-mode image. The broken line shows the intensity at 0.5% from the maximum.

B. Detection of Small Calculi Using Correlation Coefficients

Figure 4 shows a B-mode image of a calculus phantom. A specular echo returned from a polyethylene sheet just behind calculus. The echoes scattered at three calculi are not outstanding in echo intensity as compared with the specular echo. This indicates that CFAR is not suitable for small calculus detection.

We first calculated cross-correlation coefficients between IQ data of adjacent scan lines, as shown in Fig. 5. When the constant N in (1) is equal to 0, i.e. using a Wiener filter, dips in the correlation coefficients appeared around the calculus positions in the profile and extended along the range direction to the length of correlation window. However, several dips also existed at various positions. In addition, correlation coefficients are notably low in the cases where correlation windows do not contain a layered structure.

It is expected that the low correlation coefficients originated from a lack of sufficient SNR. To suppress the decrease of correlation coefficients caused by noise effects in low SNR cases, we calculated correlation coefficients using a modified Wiener filter, where the constant N is equal to $4HI_t$. When correlation windows do not contain a layered structure and signal SNR cut out by the window are expected to be low, correlation coefficients are raised to ≥ 0.8 , as shown in Fig. 6. This verified the validity of the assumption about the average noise intensity above. The modified Wiener filter also forces most dips to be inconspicuous. By contrast, three dips of correlation coefficients remained at the wire positions. These results indicate that the waveform change of transmit pulses originating from a calculus can be detected by cross-correlation between IQ data of adjacent scan lines.

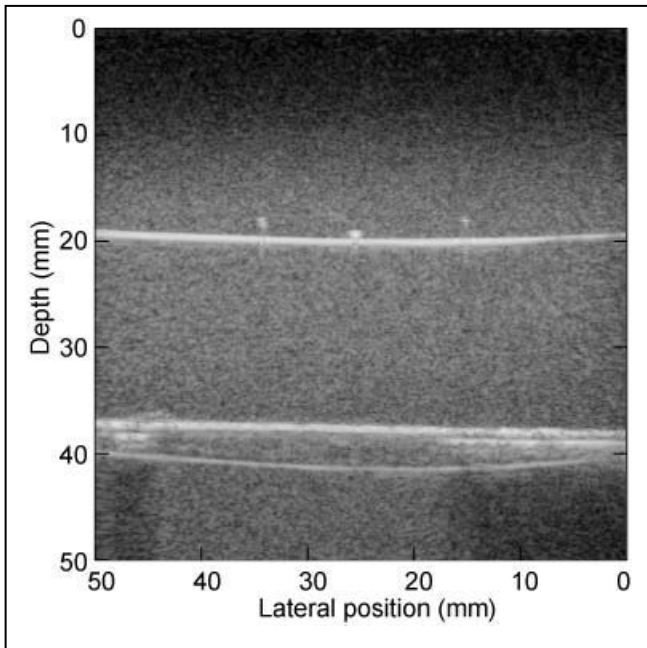


Figure 4. B-mode image of a calculus phantom.

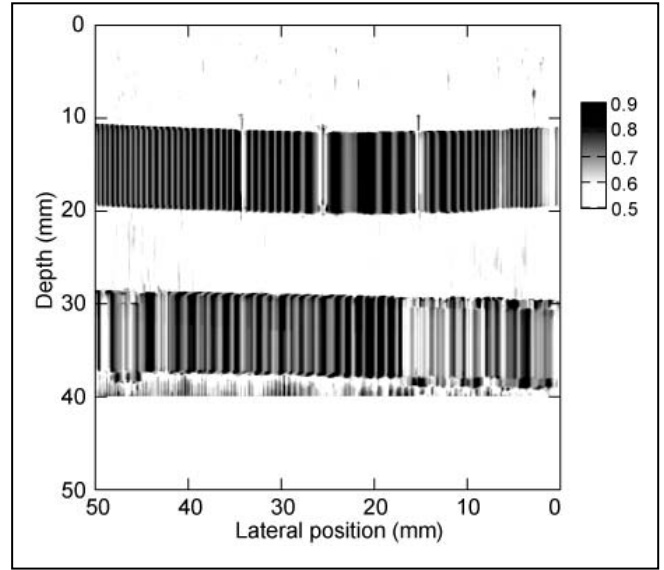


Figure 5. Correlation coefficients between IQ data of adjacent scan lines, where the constant N in (1) is equal to 0..

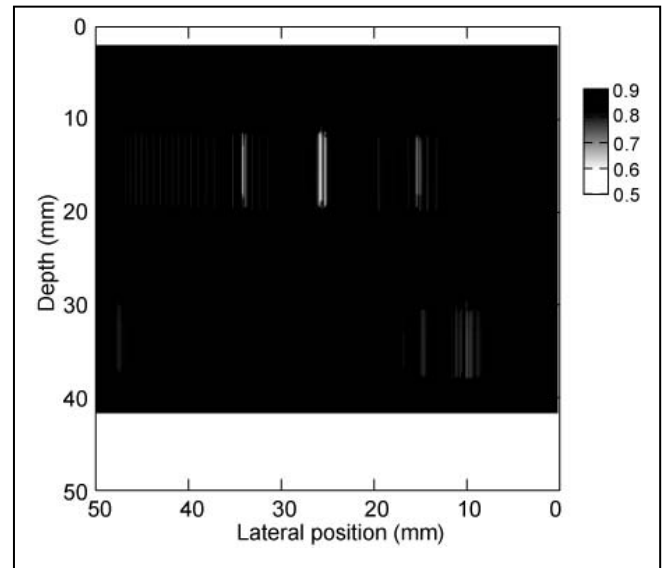


Figure 6. Correlation coefficients between IQ data of adjacent scan lines, where the constant N in (1) is equal to $4HI_t$.

V. CONCLUSIONS

We proposed a novel calculus detection method using correlation coefficients between IQ data of adjacent scan lines with a modified Wiener filter. To improve the specificity of the proposed method, we determined a proper constant to raise correlation coefficients in low SNR cases. An experimental study shows the ability of the proposed method for the detection of small calculi about 0.3 mm in diameter. This result suggests that the proposed calculus detection method has the potential to improve US tests in calculus detection.

ACKNOWLEDGMENTS

This work is partly supported by the Research and Development Committee Grants of the Japan Society of Ultrasonics in Medicine, Japan and the Innovative Techno-Hub for Integrated Medical Bio-imaging Project of the Special Coordination Funds for Promoting Science and Technology, from the Ministry of Education, Culture, Sports, Science and Technology (MEXT), Japan.

REFERENCES

- [1] H. Özdemir, M.K. Demir, O. Temizöz, H. Gençellac, and E. Unlu, "Phase inversion harmonic imaging improves assessment of renal calculi: a comparison with fundamental gray-scale sonography," *J. Clin. Ultrasound.*, vol. 36, pp.16-19, 2008.
- [2] K.A.B. Fowler, J.A. Locken, J.H. Duchesne and M.R. Williamson, "US for detecting renal calculi with nonenhanced CT as a reference standard," *Radiology*, vol. 222, pp.109-113, 2002.
- [3] H.M. Finn and R.S. Johnson, "Adaptive detection mode with threshold control as a function of spatially sampled clutter-level estimates," *RCA Rev.*, vol.29, pp.414-465, 1968.
- [4] V.G. Hansen and H.R. Ward, "Detection performance of the cell averaging LOG/CFAR receiver," *IEEE Trans. Aerosp. Electron. Syst.*, vol. 5, pp.648-652, 1972.
- [5] Y. Zhu and J.P. Weight, "Ultrasonic nondestructive evaluation of highly scattering materials using adaptive filtering and detection," *IEEE Trans. Ultrason. Ferroelect. Freq. Contr.*, vol. 41, pp.26-33, 1994.
- [6] N. Kamiyama, Y. Okamura, A. Kakee and H. Hashimoto, "Investigation of ultrasound image processing to improve perceptibility of microcalcifications," *J Med. Ultrasonics.*, vol. 35, pp.97-105, 2008.
- [7] T. Schmidt, C. Hohl, P. Haage, M. Blaum, D. Honnef, C. Weiß, G. Staatz and R. W. Günther, "Diagnostic accuracy of phase-inversion tissue harmonic imaging versus fundamental B-mode sonography in the evaluation of focal lesions of the kidney," *AJR Am. J. Roentgenol.*, vol. 180, pp.1639-1647, 2003.
- [8] E.L. Rosen and M.S. Soo, "Tissue harmonic imaging sonography of breast lesions improved margin analysis, conspicuity, and image quality compared to conventional ultrasound," *Clin. Imaging.*, vol. 25, pp.379-384, 2001.
- [9] J.F. Krücker, C.R. Meyer, G.L. LeCarpentier, J.B. Fowlkes and P.L. Carson, "3D spatial compounding of ultrasound imaging using image-based nonrigid registration," *Ultrasound med. Biol.*, vol. 26, pp.1475-1488, 2000.
- [10] A. Moskalik, P.L. Carson, C.R. Meyer, J.B. Fowlkes, J.M. Rubin and M.A. Roubidoux, "Registration of 3-dimensional compound ultrasound scans of the breast for refraction and motion correction," *Ultrasound Med. Biol.*, vol. 21, pp.769-778, 1995.